

C–H Activation of 2,4,6-Triphenylphosphinine: Synthesis and Characterization of the First Homoleptic Phosphinine–Iridium(III) Complex *fac*-[Ir(C[^]P)₃]

Leen E. E. Broeckx,[†] Wylliam Delaunay,[‡] Camille Latouche,[‡] Martin Lutz,[§] Abdou Boucekkine,^{*,‡} Muriel Hissler,^{*,‡} and Christian Müller^{*,#}

[†]Chemical Engineering and Chemistry, Eindhoven University of Technology, 5600 MB Eindhoven, The Netherlands

[‡]Institut des Sciences Chimiques de Rennes, UMR 6226 CNRS, Université de Rennes 1, Campus de Beaulieu, 35042 Rennes Cedex, France

[§]Crystal and Structural Chemistry, Utrecht University, 3584 CH Utrecht, The Netherlands

[#]Institute of Chemistry and Biochemistry, Freie Universität Berlin, Fabeckstrasse 34–36, 14195 Berlin, Germany

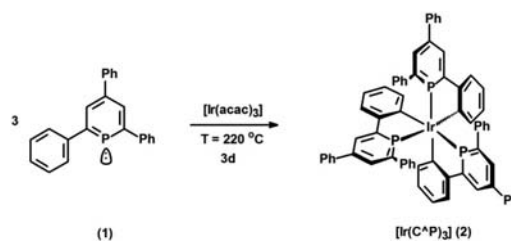
Supporting Information

ABSTRACT: Access to homoleptic phosphinine-based coordination compounds of d⁶ metals has so far remained elusive. We report here on the preparation and full characterization of the first homoleptic phosphinine–iridium(III) complex, obtained by C–H activation of 2,4,6-triphenylphosphinine with [Ir(acac)₃]. This result opens up new perspectives for the implementation of such aromatic heterocycles in more applied research fields.

The replacement of nitrogen by phosphorus in equivalent structures leads to a significant change in the electronic and steric properties of the resulting species. Phosphinines, the higher homologues of pyridines, have been shown to be particularly suitable for the stabilization of late-transition-metal centers in low oxidation states because of their weak σ -donor properties but pronounced π -accepting character. In contrast, the preparation of phosphinine complexes containing metal centers in medium-to-higher oxidation states has practically failed, while the pyridine-based counterparts are generally easily accessible.¹ Yet, access to such complexes would open up new perspectives for potential applications. In this respect, we recently discovered a new reactivity pattern of phosphinine derivatives and demonstrated for the first time that C–H activation of 2,4,6-triphenylphosphinine (**1**) by iridium(III) and rhodium(III) is possible, resulting in the corresponding complexes [Cp^{*}M(C[^]P)Cl] (M = Ir, Rh).² We attributed our findings to the chelate effect of the formally anionic bidentate P,C ligand as well as to a steric protection of the P=C double bond by the additional phenyl group in the 6 position of the phosphorus heterocycle. Inspired by these results, we set out to further explore the C–H activation of 2,4,6-triphenylphosphinine derivatives. While the Cp^{*} ligand in the precursor [Cp^{*}IrCl₂]₂ certainly represents a strong electron-donating ligand, helping to facilitate coordination of the phosphinine ligand to the formally Ir^{III} center, we were wondering whether it would be possible at all to prepare homoleptic cyclometalated complexes based on phosphinines. We envisaged that [Ir(C[^]P)₃] (**2**) could be an interesting target molecule because the analogous nitrogen-

based systems [Ir(C[^]N)₃] (C[^]N = cyclometalated 2-arylpyridine derivative) are well-known.³ However, such complexes are generally synthesized in multistep procedures using IrCl₃·H₂O and 2-arylpyridines as starting materials in combination with high-boiling alcohols and/or water to optimize yields and selectivity.³ Unfortunately, both the metal precursor and reaction conditions are generally not compatible with phosphinines because the P=C double bond is usually sensitive toward nucleophilic attack by protic solvents.² Moreover, we realized that coordinating up to three bulky 2,4,6-triphenylphosphinines to the Ir^{III} center might be difficult to achieve. Nevertheless, we decided to attempt the ortho metalation of **1** with [Ir(acac)₃] and ultimately performed the reaction in a sealed autoclave under rather harsh reaction conditions at T = 220 °C for 3 days (Scheme 1).

Scheme 1. Synthesis of **2**



Interestingly, orange crystals could be isolated from the reaction mixture, and the ³¹P NMR spectrum of the product showed a single resonance at δ 167.6, indicating that the thermodynamically more stable *fac* isomer of **2** had been formed selectively. Matrix-assisted laser desorption/ionization time-of-flight analysis revealed an *m/z* ratio of 1160.21 g/mol, demonstrating that the tris-cyclometalated product had indeed been formed. Crystals of **2** suitable for X-ray diffraction could further be obtained by slowly evaporating the solvent of a solution of **2** in toluene, and the X-ray crystal structure

Received: July 29, 2013

Published: September 10, 2013

unambiguously confirmed the formation of complex **2**. *fac*-[Ir(C[^]P)₃] crystallizes in the noncentrosymmetric space group *P*2₁ (No. 4) with three independent molecules in the asymmetric unit (two Δ and one Λ isomers in the measured crystal), and the molecular structure of one Δ isomer is shown in Figure 1 (see also the Supporting Information, SI).

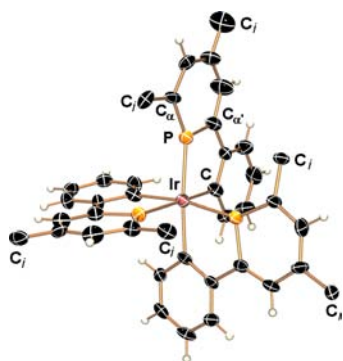


Figure 1. Molecular structure of *fac*- Δ -**2** in the crystal. Displacement ellipsoids are shown at the 50% probability level. Only one of three independent molecules is represented. The phenyl substituents in the 4 and 6 positions of the heterocycle have been omitted for clarity, and only the corresponding *ipso*-C (C_i) atoms are shown.

The molecular structure of **2** shows a distorted octahedral coordination geometry around the Ir^{III} center. The Ir–P and Ir–C bond distances are in the ranges of 2.259(2)–2.280(18) and 2.129(7)–2.158(7) Å, respectively. As expected, the metal center is not located in the ideal axis of the phosphorus lone pair because of the larger size of the phosphinine heterocycle compared to pyridine. Much to our surprise, it further turned out that **2** is air- and moisture-stable. A space-filling model of **2** (see the SI) shows that the P=C double bonds are rather inaccessible for reactions with protic reagents. In fact, the additional phenyl groups in the 4 and 6 positions of the heterocyclic framework create an organic shell around the inner core of the complex, presumably resulting in a kinetically very stable compound.

In order to establish structure–property relationships, the optical and redox properties of **2** were investigated in CH₂Cl₂. The absorption spectrum presents an intense band centered at $\lambda = 289$ nm along with a red-shifted broad intense absorption band extending from $\lambda = 315$ to 405 nm (Figure 2). This spectrum differs from the one recorded for **1**, which presents an intense band centered at $\lambda = 279$ nm along with a red-shifted shoulder tailing down to $\lambda = 345$ nm (Figure 2).⁴ For rationalization of the

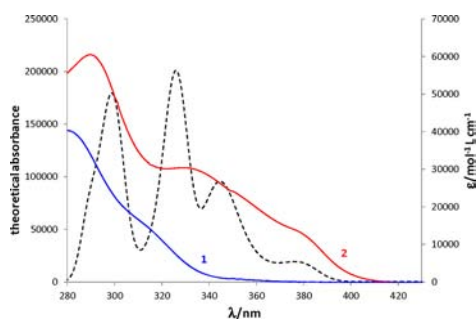


Figure 2. Absorption spectra of **1** (continuous blue line) and **2** (continuous red line) in CH₂Cl₂ and TD-DFT-simulated spectrum of **2** (dashed black line).

observed properties, density functional theory (DFT) and time-dependent DFT (TD-DFT) calculations were carried out on phosphinine **1** as well as on complex **2**, and the orbital and atomic percentage compositions of the frontier molecular orbitals (MOs) are given in Table 1. It is worth noting that the

Table 1. Percentage Orbital or Atomic Weights of Relevant Moieties in Frontier MOs^a of **1** and **2**

	MO	H-4	H-3	H-2	H-1	H	L	L+1	L+2
1	PC ₅ H ₂ ^b		9	10	39	59	73	63	
	P		7	3	1	33	36	2	
2	Ir d	14	13	6	6	19	4	3	2
	Ir ^c	14	13	6	6	19	6	4	3
	3P ^d	6	6	19	21	17	32	31	30
	3(PC ₅ H ₂)	6	7	20	31	26	42	54	53

^aH = HOMO; L = LUMO. ^bTotal phosphinine contribution. ^cTotal iridium contribution. ^dTotal phosphorus contribution.

computed structural data for **2** are very similar to those obtained by the X-ray diffraction study (for details, see the SI). Analysis of the ligand MOs (**1**) shows that the highest occupied MO (HOMO) and lowest unoccupied MO (LUMO) are mainly localized at the phosphinine core, with more than 30% contribution of the P atom. The TD-DFT calculations performed on **1** assign the computed band at $\lambda = 315$ nm (shoulder experimentally) to a HOMO \rightarrow LUMO transition, corresponding to an intra-phosphinine charge transfer (Table 1 and Figure 3) with a strong contribution of the P atom (see also the SI).

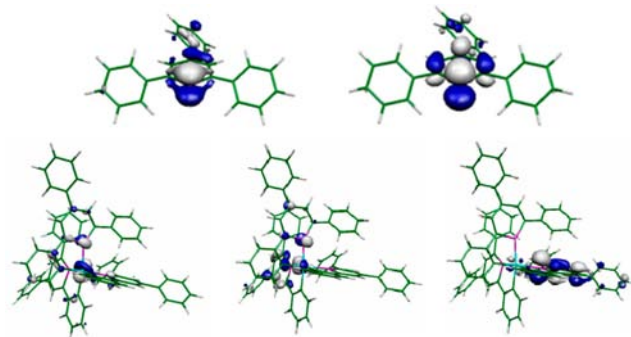


Figure 3. HOMO and LUMO of **1** (top) and HOMO, LUMO, and LUMO+1 of **2** (bottom).

Because this transition is weakly allowed, only a low fluorescence intensity is observed at $\lambda = 430$ nm (quantum yields $\ll 1$), which is nicely reproduced by TD-DFT computations ($\lambda = 403$ nm).⁵ The absorption band at $\lambda = 279$ nm (computed at $\lambda = 290$ nm) can be assigned to a mix of HOMO \rightarrow LUMO+1 and HOMO–1 \rightarrow LUMO transitions, which are mainly π – π^* and n – π^* charge transfers and particularly from the P atom to the hydrocarbon part of the phosphinine.

Considering complex **2**, it is worth noting that the frontier MOs from HOMO–2 to LUMO+2 exhibit significant phosphinine and P atom character (Table 1). Moreover, the weight of the Ir 5d orbitals is important in HOMO, HOMO–3, and HOMO–4, which most likely allow the occurrence of metal-to-ligand charge-transfer (MLCT) absorption bands. In the simulated absorption spectrum of complex **2** (Figure 2), the

computed absorption band of the highest energy at $\lambda = 298$ nm fits nicely with the observed one at $\lambda = 289$ nm. This absorption band, which originates mainly from HOMO-7 \rightarrow LUMO and HOMO-6 \rightarrow LUMO transitions (SI), corresponds to electron density transfer from phenyl groups to phosphinine cores. The second absorption band observed at ca. $\lambda = 335$ nm corresponds to the calculated excitations at $\lambda = 326$ and 346 nm. The originating electronic transitions, among them HOMO-3 and HOMO-4 to LUMO, which exhibit the highest oscillator strengths (SI), are mainly MLCT involving particularly an electron transfer from the metal to phosphinine ligands. Finally, the observed shoulder at ca. $\lambda = 385$ nm fits rather nicely with the calculated one at $\lambda = 376$ nm, corresponding to a HOMO \rightarrow LUMO transition with a low oscillator strength. It can be assigned to an MLCT with a significant metal-to-phosphinine electron transfer (Figure 3).

A degassed solution (methyltetrahydrofuran or CH_2Cl_2) of **2** when excited in the MLCT low-energy absorption band at 298 K shows a very weak emission intensity centered at $\lambda = 430$ nm, resembling the ligand fluorescence. Indeed, this value again fits well with the fluorescence emission at ca. $\lambda = 410$ nm computed theoretically by TD-DFT. Negligible changes of the emission intensity were observed upon aeration of the solution, likely indicating that the emission is mainly ligand-centered and does not originate from a $^3\text{MLCT}$ triplet state. Moreover, no further emissions were detected at low temperature. These photo-physical data indicate that radiationless deactivation pathways are mainly responsible for deactivation of the excited states. At the moment, a straightforward explanation for the nonemissive property of complex **2** still remains elusive, except for the low oscillator strength of the MLCT excitations. As a matter of fact, specific features to rationalize the lack of phosphorescence of transition-metal complexes are missing in our case.⁶ Among those are the inefficiency of spin-orbit coupling, i.e., high-energy differences between occupied Ir 5d orbitals or low-energy differences between occupied and vacant Ir 5d orbitals, as well as low 5d metal orbital contributions within the HOMOs in the lowest $^3\text{MLCT}$ state and an important distortion of the geometry of this triplet state. Furthermore, the TD-DFT calculations showed that the HOMOs have an important contribution of both phosphinine and metal character, leading to a mixing of various types of transitions (MLCT, intraligand charge transfer, and/or ligand-to-ligand charge transfer) in the excited state, which might induce radiationless deactivation.⁶

In order to gain more insight into the electronic structures of **1** and **2**, their electrochemical properties were further investigated by means of cyclic voltammetry (CH_2Cl_2 , 0.2 M Bu_4NPF_6 , and $\nu = 200$ mV/s) using ferrocene as the internal standard. **2** undergoes two irreversible electronic oxidation and reduction waves ($E^{\text{ox}1} = +0.74$ V; $E^{\text{ox}2} = +1.11$ V; $E^{\text{red}1} = -2.17$ V; $E^{\text{red}2} = -2.34$ V vs Fe), while **1** shows only an irreversible cathodic peak potential at -1.40 V in the studied electrochemical window.⁷ At this stage, we believe that the oxidation occurs mainly at the metal site, along with minor contributions from the ligand. Furthermore, and in contrast to the oxidation process, the reduction may occur primarily on the low-lying π^* orbitals of the ligand.⁷ This assignment is supported by the frontier MO diagram of the complex (see the SI). The electrochemical measurements show that **2** is easier to reduce and more difficult to oxidize compared the reference compound $[\text{Ir}(\text{C}^{\wedge}\text{N})_3]$, indicating that the phosphinine ligand **1** induces a stabilization of the LUMO and HOMO of complex **2** because it is a better π acceptor than the corresponding pyridine ligand.^{1,8}

In summary, we successfully isolated and crystallographically characterized the first homoleptic phosphinine-iridium(III) complex $\text{fac-}[\text{Ir}(\text{C}^{\wedge}\text{P})_3]$, which was prepared by C-H activation of 2,4,6-triphenylphosphinine with $[\text{Ir}(\text{acac})_3]$. First investigations on the physical properties and TD-DFT calculations of **2** showed that this complex does not show any phosphorescence emission. Nevertheless, our here-described first results offer new perspectives for the application of phosphinine-based coordination compounds in molecular materials science. Currently, experiments are being performed in our laboratories to carefully optimize the structure of the ligand and to avoid mixing of various types of transitions.

■ ASSOCIATED CONTENT

Supporting Information

Synthetic procedure, complete characterizations, X-ray crystallographic data and CIF file for **2**, and computational details. This material is available free of charge via the Internet at <http://pubs.acs.org>.

■ AUTHOR INFORMATION

Corresponding Authors

*E-mail: abdou.boucekkine@univ-rennes1.fr.

*E-mail: muriel.hissler@univ-rennes1.fr.

*E-mail: c.mueller@fu-berlin.de.

Notes

The authors declare no competing financial interest.

■ ACKNOWLEDGMENTS

This research is supported by The Netherlands Organization for Scientific Research (NWO), Ministère de la Recherche et de l'Enseignement Supérieur, University of Rennes 1, CNRS, IUF. The COST CM0802 (Phoscinet) and PHC Van Gogh Programme are also acknowledged.

■ REFERENCES

- (1) (a) Müller, C.; Broeckx, L. E. E.; de Krom, I.; Weemers, J. J. M. *Eur. J. Inorg. Chem.* **2013**, 187. (b) Mézailles, N.; Mathey, F.; Le Floch, P. *Prog. Inorg. Chem.* **2001**, 49, 455.
- (2) Broeckx, L. E. E.; Lutz, M.; Vogt, D.; Müller, C. *Chem. Commun.* **2011**, 47, 2003.
- (3) (a) You, Y.; Nam, W. *Chem. Soc. Rev.* **2012**, 41, 7061. (b) Endo, A.; Suzuki, K.; Yoshihara, T.; Tobita, S.; Yahiro, M.; Adachi, C. *Chem. Phys. Lett.* **2008**, 460, 155. (c) Nazeeruddin, M. K.; Humphry-Baker, R.; Berner, D.; Rivier, S.; Zuppiroli, L.; Graetzel, M. *J. Am. Chem. Soc.* **2003**, 125, 8790.
- (4) Dimroth, K. *Top. Curr. Chem.* **1973**, 38, 1.
- (5) Müller, C.; Wasserberg, D.; Weemers, J. J. M.; Pidko, E. A.; Hoffmann, S.; Lutz, M.; Spek, A. L.; Meskers, S. C. J.; Janssen, R. A.; van Santen, R. A.; Vogt, D. *Chem.—Eur. J.* **2007**, 13, 4548.
- (6) (a) Manuta, D. M.; Lees, A. J. *Inorg. Chem.* **1986**, 25, 1354. (b) Demas, J. N.; DeGraf, B. A. *Anal. Chem.* **1991**, 63, 829B. (c) Yang, C.-H.; Li, S.-W.; Chi, Y.; Cheng, Y.-M.; Yeh, Y.-S.; Chou, P.-T.; Lee, G.-H.; Wang, C.-H.; Shu, C.-F. *Inorg. Chem.* **2005**, 44, 7770.
- (7) Le Floch, P.; Carmichael, D.; Ricard, L.; Mathey, F.; Jutand, A.; Amatore, C. *Organometallics* **1992**, 11, 2475.
- (8) Dedeian, K.; Shi, J.; Shepherd, N.; Forsythe, E.; Morton, D. C. *Inorg. Chem.* **2005**, 44, 4445.